Design and Evaluation of a Thermal Precipitation Aerosol Electrometer (TPAE)

Shipeng Kang[1,2], Tongzhu Yu[1], Yixin Yang[1], Jiguang Wang[5,6], Huaqiao Gui[1,2,4], Jianguo Liu[1,2,4], Da-Ren Chen[3]

5   [1]Key Laboratory of Environmental Optics and Technology, Anhui Institute of Optics and Fine Mechanics, Hefei Institutes of Physical Science, Chinese Academy of Sciences, Hefei 230031, China

[2]University of Science and Technology of China, Hefei 230026, China

[3]Particle Laboratory, Department of Mechanical and Nuclear Engineering, Virginia Commonwealth University, Richmond, VA 23284, USA

10   [4]Innovation excellence Center for Urban Atmospheric Environment, Institute of Urban Environment, Chinese Academy of Science, Xiamen 361021, China

[5]China Automotive Technology and Research Center Co., Ltd, No.68 Xianfeng East road, Dongli District, Tianjin, 300300, China

[6]CARARC Automotive Test Center (Kunming) Co., Ltd, No.68 Donghuan road, Kunming, 651701, China

15   *Correspondence to*: Da-Ren Chen (dchen3@vcu.edu), Tongzhu Yu (tzyu@aiofm.ac.cn)

Abstract. A new aerosol electrometer, the Thermal Precipitation Aerosol Electrometer (TPAE), was designed for use with particles of sizes less than 300 nm and its performance was experimentally evaluated. The TPAE combines the thermal precipitator with a micro-current measurement circuit board (i.e., pre-amp) for measuring the current carried by collected particles. The thermal precipitator is in the disk-to-disk configuration. Heating paster and air cooling were adopted to establish

20   the desired temperature gradient in the precipitation chamber. At a sample flow rate of 0.3 L/min and a temperature gradient of 264K/cm, the precipitation efficiency of 70 nm particles reaches ~100%. The measurement range of the designed aerosol electrometer is $\pm 5 \times 10^5$ fA, and the accuracy is ± 2fA ($2500\#/cm^3 \sim 6.25 \times 10^7 \#/cm^3$ using a flowrate of 0.3 L/min and assuming only singly charged particles exist in the sample). During the evaluation process, the electrical performance of the TPAE was first tested using sodium chloride (NaCl) and soot particles previously classified by a differential mobility analyzer

25   (DMA) and compared to the reference. The precipitation performance of the TPAE was then characterized as functions of the temperature gradient, sampling flowrate, and particle size. It was shown that the particle collection efficiency of the built-in thermal precipitator is inversely proportional to the sampling flow rate, and proportional to the temperature gradient. The effect of particle size on the particle collection efficiency was minor for NaCl particles of sizes between 23 to 200 nm. Unlike that which was observed for the NaCl particles, a slightly positive correlation between the collection efficiency and the mobility

30   size for soot particles (in the size range of 30 ~ 160 nm) was observed. This observation might be due to the existence of soot agglomerates. Compared to existing electrometers, the TPAE does not require the use of high efficiency filters and includes the additional feature of the "soft" collection of particles for offline particle characterization as well as aerosol current measurement.

1 Introduction

35   Instruments for measuring the integral parameters of aerosol particles, e.g., the total number, surface area, and mass concentration of particles, are important for the characterization of particulate matter (PM) emitted from various PM sources. Example applications of such instruments include the measurement of vehicle particle emissions (Faxvog et al., 2007, Kheirkhah et al., 2020), ocean aerosols (Held et al., 2011), atmospheric aerosols (Hillemann et al., 2014) and urban particles (Molgaard et al., 2013, Etzion et al., 2018, Alas et al., 2019). Furthermore, such measurement instruments could be combined

40   with a size/mobility classifier, e.g., differential mobility analyzers (DMAs), for measuring the size distribution of aerosol particles. An example of the above is electrical mobility particle sizers, which are widely applied for measuring the size distribution of fine and ultrafine particles.

Condensation particle counters (CPCs) and aerosol electrometers (AEs) are both typically used for the characterization of the total number concentration of aerosol particles. CPCs count the number of particles over a given time by enlarging the particle

45   size (via condensation of the working fluid vapor) and counting them one-by-one (via optical means). The single particle counting process of CPCs makes them suitable for measuring the number concentration of particles, particularly at low concentrations. CPCs have also been combined with DMAs (as scanning mobility particle sizers or SMPSs) to measure the size distribution of sub-micrometer-sized particles. The measurement task described above can also be accomplished by electrical means, where particles are first required to be electrically charged. The charge/current carried by the aerosol particles

50   is then measured by an aerosol electrometer (AE). Therefore, aerosol charges are required to work with AEs to measure the number concentration of particles (i.e., with the known average charges on particles provided by the charger). Another important usage of AEs is to calibrate the performance of CPCs using DMA-classified particles (Giechaskiel et al., 2009). A commercial version of the aerosol electrometer is the TSI Model 3068B. Note that the charger-AE assembly in that model has been applied to measure the total mass/surface area concentration of particles. However, the measurement tasks were

55   accomplished by empirical calibration of the assembly responses via selected calibration particles. The calibration curves may be varied when measuring particles with the composition different to that of calibration particles.

A Faraday Cup equipped with a high efficiency filter is typically used in aerosol electrometers to collect sampled particles and to induce the current resulting from the continuous collection of charged particles. Yang et al. (2018) developed an aerosol electrometer in which particles were collected by a metal filter and then the current carried by particles was directly measured

by a micro current measurement circuit (i.e., pre-amp) through a copper probe. The miniDiSC (Diffusion Size Classifier) developed by Fierz et al. (2018) used two filter stages to collect particles of different sizes, in which a porous metal filter is used in the first stage to collect small particles. Liu et al. (2020) developed a mini-eUPS (electrical Ultrafine Particle Sizer) in which a miniature aerosol electrometer was used after a plate electrical mobility classifier to detect the current carried by DMA-classified particles. A TEOM (Tapered Element Oscillating Microbalance) filter disk is used in the mini aerosol electrometer. Seol et al. (2000) developed a Faraday Cup electrometer for operation at 200-930 Pa of pressure, in which porous metal mesh and filters are used for collecting charged particles. Intra et al. (2014) used an aerosol electrometer to measure atmospheric ions and charged particles, in which the particle collection was achieved using a HEPA filter.

Charged particles could also be collected by inertial impaction on electrically isolated metal substrates, from which the current from the continuous collection of charged particles can be directly measured. An example of an instrument that uses such a technique is the Electrical Low-Pressure Impactor (ELPI) (Keskinen et al., 1992). Another method charged particles can be collected by is through electrical precipitation, such as what is used in the Engine Exhaust Particle Sizer (EEPS) reported by Tammet et al. (2002) and Wang et al. (2016). Electrostatic precipitation is also used in aerosol samplers for off-line characterization of collected particles. Nanometer aerosol sampler (TSI model 3089; Dixkens and Fissan, 1999) is one example of such an aerosol sampler. The collection of charged particles either by filtration, inertial impaction, or electrical means makes it possible to alter the morphology of collected particles, particularly for particle agglomerates (e.g., soot particles). However, the methods above are not favored for offline SEM analysis of particles, if required.

Compared to the collection methods described above, the collection of particles by thermal precipitation is a good candidate for the "soft" collection of particles, e.g., disk (Kethley et al., 1952, Wang et al., 2012), plate-to-plate (Tsai and Lu, 1995) and cylindrical thermal precipitator (Bredl and Grieve, 1951, Wang et al., 2012). Furthermore, the minor particle size effect on particle collection by thermal precipitation (for particles of sizes less than 300 nm) has been documented (Wang et al., 2012). Note that collection by inertial impaction favors inertial particles, and electrical collection favors diffusive particles. The effectiveness of both collection methods depends significantly on the particle size.

In a thermal precipitator, particles are introduced into a precipitation zone in which a temperature gradient is established. The direction of the temperature gradient is typically perpendicular to that of the flow direction. Once the particles enter the precipitation chamber, the thermophoretic force moves the particles from the hot plate to the cold plate, and the particles eventually precipitate. If the cold plate is well insulated from other metal structures, it could serve as an electrode for current measurement, which also favors the cold environment due to the reduction of thermal noise. However, the cold plates of existing thermal precipitators cannot be directly connected to an electrometer due to poor electrical insulation. The structure and cooling methods of thermal precipitators must be re-designed for integrating thermal precipitation particle collection with the measurement of the aerosol current.

The objective of this work is thus the development of a thermal precipitation aerosol electrometer (TPAE), combining both

thermal precipitation with current measurement for charged particles in one device. The overall performance of the prototype was experimentally calibrated and compared to that offered by Faraday Cup aerosol electrometers. For the electrical performance evaluation, the zero-point and response time of the electrometer was calibrated, and the linear correlation of readouts of the TPAE and the reference was examined. For the thermal precipitation performance, the collection efficiency of the TPAE was investigated as functions of the temperature gradient, sampling flow rate and particle sizes. NaCl particles and soot particles were used as test particles.

2 Design of Thermal Precipitation Aerosol Electrometer
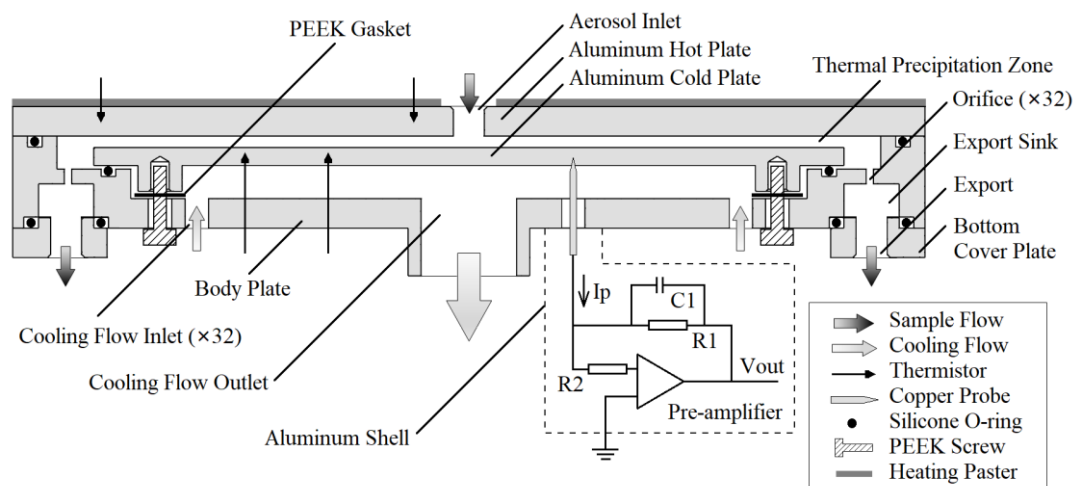
Fig 1: Schematic diagram of the protype Thermal Precipitation Aerosol Electrometer (TPAE)

Fig. 1 shows the schematic diagram of the thermal precipitation aerosol electrometer (TPAE). The TPAE consists of two parts: one part for the thermal deposition of particles and the other for the measurement of current carried by collected particles. The thermal precipitation part is in the disk-to-disk configuration. Sampled aerosol particles enter the precipitation chamber from the inlet tube located at the disk center, radially flow outwards in the space defined by two separated and centered disks, and eventually exit through a series of evenly distributed holes (at the outer diameter of the disks) to a circumferential chamber designed at the disk edge. A temperature gradient is established between two aluminum disks (with the top disk heated and the bottom disk cooled). The spacing between the two disks is controlled by PEEK gaskets. To improve the precipitation efficiency of particles and reduce the size of the TPAE, the constructed thermal precipitation chamber is 0.5 mm in gap distance and its diameter is 120 mm. In the thermal precipitation chamber, the temperature gradient deflects the motion of sampled particles from the flow. The top disk is heated by attaching a heating paster on its outside, while the cold disk is cooled by air flowing in the chamber underneath the precipitation chamber (i.e., air-cooling chamber). Driven by the suction from the outlet of the air-cooling chamber, the cooling air enters the chamber through a series of holes located close to the chamber's outer diameter. The flow rate of cooling air (~20 lpm) is monitored by a mass flow meter (Beijing Sevenstar Flow, Model CS100). Four thermistors (Songtian Electronics, 100KΩ) were used to measure the temperatures of the heat and cold disks.

115 A spring-loaded solid copper pin is attached to the cold disk for measuring the current carried by the collected particles. With the above arrangement, the cold disk serves as the electrode for the current measurement and is enclosed in the cage formed by the hot metal plate and the air-cooling chamber, protecting the pre-amp from potential electromagnetic interference. Note that the copper pin is exposed to the cooling air, and the thermal noise of the pre-amp can also be reduced if cold air is used. As shown by the dashed line in Fig. 1, the current carried by the charged particles was measured through a R_1 resistor of

120 $10G\Omega$ so that V_{out} at the output pin of the pre-amplifier (ADA4530-1) can be calculated using the current. The supply voltage of the pre-amplifier is ±5 V, resulting in the measuring range of the TPAE being $\pm5V/10G\Omega = \pm5\times10^5$ fA. A capacitor C_1 (47pF) was used to suppress the noise bandwidth. The current and the number of sampled particles (assuming all the particles are carrying the same charges) can be calculated using Eqs. (1) and (2), where ΔI_p is the increment of discharge current, ΔV_{out} is the increment of the pre-amplifier output, ΔN_p is the increment of the number of collected particles, e is elementary charge,

125 x is the average charge of the charged particles (determined by an aerosol charger, which is not a part of the TPAE), and η is the particle collection efficiency.

$$\Delta I_p = -\frac{\Delta V_{out}}{R_1} \ , \tag{1}$$

$$\Delta N_p = \frac{\int \Delta I_p dt}{ex\eta} \ , \tag{2}$$

In practical terms,

130 $$\begin{cases} \Delta I_p = I_{pm} - I_0 \\ \Delta V_{out} = V_{outm} - V_0 \ , \\ \Delta N_p = N_{pm} - N_0 \end{cases} \tag{3}$$

where I_{pm}, V_{outm} are measured values while I_0, V_0 and N_0 are the null point value of the thermal precipitation aerosol electrometer. The zero-point, x, η are parameters to be determined by experiments. To calculate N_{pm} in the measurements, the zero-point must be measured under the charged-particle-free flow condition (i.e., with a HEPA filter placed at the inlet of the TPAE).

3 Experimental Setup and Data Analysis

135

To evaluate the performance of the TPAE, the basic performance of the electrometer and the particle collection efficiency of the thermal precipitation zone must first be investigated. The basic performance of the electrometer includes the zero-point, the low response time, and its output linearity with the readout of a reference electrometer.

3.1 Experiment Setup
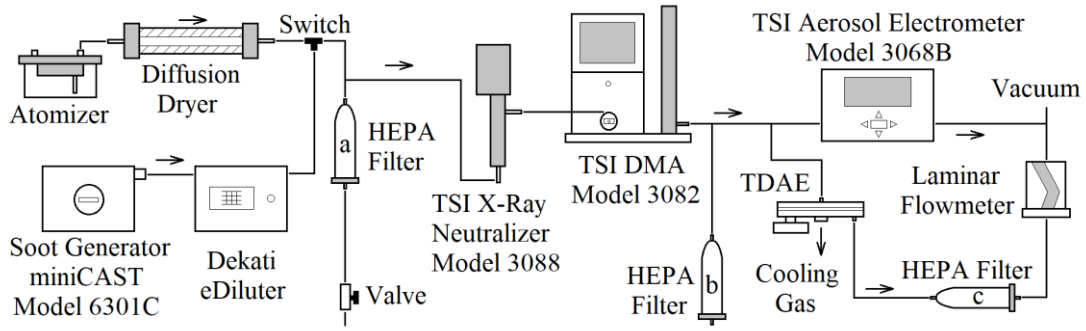
Fig 2: Schematic diagram of experimental setup for the TPAE performance evaluation

Fig. 2 shows the schematic diagram of the experimental setup to investigate the performance of the TPAE. The aerosol electrometer (TSI Model 3068B) was selected as the reference in the setup. NaCl droplets were generated by the atomizer (TSI Model 9302) with aqueous NaCl solutions of 0.005 g/ml and a diffusion-type dryer was used to remove the water in droplets. Soot particles were generated by a soot generator (Jing, Model miniCAST 6301C) with propane as the fuel. A diluter was applied to reduce the soot particle concentration. A differential mobility analyzer (DMA, TSI Model 3082) was utilized to classify test particles of selected electrical mobility sizes. Particles entering the DMA were passed through a soft X-ray aerosol charger (TSI Model 3088). A bypass line with a HEPA filter and a valve was included preceding the charger to make sure the desired flow rate was entering the charger and the DMA. The prototype and a Faraday Cup aerosol electrometer (TSI Model 3068B) were set up in parallel connected downstream of the DMA. The other bypass line with a HEPA filter was also included to ensure the total flowrate required for operation of the prototype and reference electrometer. The sampled particle-laden flow was driven by a vacuum pump and monitored by a laminar flowmeter. The sampled particle flow after the TPAE was passed through a HEPA filter to remove any uncollected particles prior to the laminar flowmeter. The cooling air of the TPAE was driven by suction from the outlet of the cooling air chamber via a pump. A vacuum pump was connected to the TSI aerosol electrometer to drive its flowrate. Note that the sampling flow rates of the TPAE and the TSI electrometer were kept the same in the experiments.

The V_{outm} of the TPAE was then converted to digital signals, which were sent to a PC so that I_{pm} could be recorded in real time at 4 Hz and averaged to 1 Hz.

3.2 Experimental design

3.2.1 Measurement of Zero-point

A stable zero-point is the basis for any current measurement by an electrometer. A high fluctuation of the zero-point increases the threshold signal-to-noise ratio, making the measurement less sensitive, and a drifting of the zero-point results in inaccurate measurements. An experiment using the setup described in the previous section was carried out to measure the zero-point trend during the warm-up of the TPAE. In this part of the experiments, the air flow was entirely provided by the bypass line installed

165 after the DMA, which was accomplished by shutting down the soot generator and valve in the bypass line installed before the soft X-ray aerosol charger. The sampling flow rates of the TPAE was set at 0.3 L/min. The cooling air flow rate was at ~20 L/min. According to preliminary experiments, particles of sizes smaller than 100 nm were totally collected under this setting (thus it was set to be the typical TPAE working condition). Note that, due to the fact that the zero-point varies based on the ambient temperature and many other environmental factors, it is measured prior to each test measurement.

3.2.2 Experiment of Response Time

A step response experiment was performed to measure the response time of the TPAE. For an aerosol electrometer, the response time is affected by the rate of particle collection and the performance of pre-amp. In this part of the calibration, the soot generator was used. The temperature gradient of the TPAE was set at 264 K/cm. The sample flowrates of the TPAE and the TSI aerosol electrometer were kept at either 0.3 L/min or 0.6 L/min. The response time of the TPAE was tested under two working settings, i.e., at 0.3 L/min to study the full precipitation efficiency (~ 100%), and at 0.6 L/min for the low collection efficiency. After the two aerosol electrometers were warmed up, a switch valve (installed between the atomizer and soot generator lines) was used to manually impose a step change in the number concentration of soot particles. The DMA was set to classify soot particles with electrical mobility size of 70 nm.

3.2.3 Investigation of the linearity of two aerosol electrometer readouts

This part of the experiment calibrated the readout linearity of both the TPAE and the TSI aerosol electrometer. The collection efficiency of the HEPA filter used in the TSI aerosol meter is close to 100%. The particle collection efficiency of the TPAE was assumed to be constant with the given temperature gradient and sampling flowrate according to previous works (Wang et al., 2012). For this calibration, soot particles of various concentrations were produced. The electrical mobility size of test particles was 70 nm (classified by the DMA). The temperature gradient of the TPAE was maintained at 264 K/cm and the sampling flow rates of the TPAE and the TSI aerosol electrometer were both set at 0.3 L/min. For each test concentration, the average of the readouts in one minute was reported for the comparison.

3.2.4 Study of the particle collection Efficiency of TPAE

For this part of study, the collection efficiency of the TPAE was measured as the function of the sampling flowrate, temperature gradient, and electrical mobility size, i.e., $\eta(Q_{in})$, $\eta(\overrightarrow{\nabla T})$ and $\eta(d_p)$, respectively, where $\overrightarrow{\nabla T}$ is the temperature gradient of thermal precipitation field, d_p is the electromigration particle diameter and Q_{in} is the sampling flow rate. For the measurements of $\eta(Q_{in})$ and $\eta(\overrightarrow{\nabla T})$ of the prototype, sodium chloride particles with electrical mobility diameters ranging from 23 ~ 200nm were tested, while for $\eta(d_p)$, both sodium chloride and soot particles were tested.

By keeping the same length of transport tubes connecting the DMA exit to both the TPAE and the TSI aerosol electrometer, it was assumed that the particle loss in the tubes were the same since the sampling flow rate of both electrometers was kept the

same for a given test. The collection efficiency, η, was then calculated by Eq. (4), where I_s is the current measured by the TSI aerosol electrometer.

$$\eta = \frac{I_{pm} - I_0}{I_s} \,,\tag{4}$$

The temperature gradient, $\overrightarrow{\nabla T}$, was calculated by Eq. (5), where W is the gap distance of the thermal precipitation zone, and the direction of $\overrightarrow{\nabla T}$ is perpendicular to the disks (from the hot one to the cold one).

$$\left|\overrightarrow{\nabla T}\right| = \frac{T_{hot} - T_{cold}}{W} \,,\tag{5}$$

Varying the $\overrightarrow{\nabla T}$ was done by changing the cooling flowrate. The electrical mobility diameters, d_p, of the test particles was determined by the DMA operation, whose ratio of sheath flow to aerosol sampling flowrates was 4:1. The sampling flowrate of the TPAE, Q_{in}, was controlled by a valve and monitored by a laminar flowmeter. Table 1 summarizes the experimental conditions for this part of study.

Table 1: Experimental conditions for the measurements of TPAE collection efficiency

Measured	Experimental Condition			
	d_p (nm)	$\left|\overrightarrow{\nabla T}\right|$ (K/cm)	Q_{in} (L/min)	Material
$\eta(Q_{in})$	70, 200	254	0.3 ~ 1.0	NaCl
$\eta(\overrightarrow{\nabla T})$	70	160 ~ 310	0.3, 0.6	NaCl
$\eta(d_p)$	23 ~ 200	254	0.3, 0.6	NaCl, Soot

3.3 Model for the particle collection efficiency of thermal precipitation

To validate the measured particle collection efficiency of the TPAE, we applied the model developed by Wang et al. (2012) to calculate the thermal deposition efficiency of thermal precipitators in the disk-to-disk configuration and compared them to our measurements. The details of the model can be found in the work of Wang et al. (2012). A summary of the model is given for reference. Assuming that the flow is steady-state, incompressible, laminar and axisymmetric, and that particles are evenly distributed at the entrance, the collection efficiency of thermal precipitators in the disk configuration can be calculated as

$$\eta = \frac{\pi r^2 V_{th}}{Q_{in}} \,,\tag{6}$$

where Q_{in} is the aerosol sampling flowrate, r the radius of the precipitation disk, and the thermal velocity, V_{th}, which is calculated as

$$\vec{V}_{th} = \frac{\mu \overrightarrow{\nabla T} H C_c}{\rho_g T} \,,\tag{7}$$

in which $\overrightarrow{\nabla T}$ is the temperature gradient, T is the absolute temperature of particles, ρ_g is the density of carry gas, and H is

the thermophoretic coefficient. According to Talbot et al. (1980), H can be calculated by Eq. (8), where k_g and k_p are the conductivity of air and the particle. $C_s = 1.147$, $C_t = 2.20$ and $C_m = 1.146$ are constants. C_c is the Cunningham correction factor calculated by Eq. (9).

$$H = \frac{2C_s(\frac{k_g}{k_p}+C_tK_n)}{(1+3C_mK_n)(1+\frac{2k_g}{k_p}+2C_sK_n)} , \tag{8}$$

$$\begin{cases} C_c = 1 + K_n[\alpha + \beta \exp\left(-\frac{\gamma}{K_n}\right)] \\ K_n = \frac{2\lambda}{d_p} \end{cases} , \tag{9}$$

where $\alpha = 1.142$, $\beta = 0.558$, $\gamma = 0.999$, K_n is Knudsen number and λ is the mean free path of air.

According to Eq. (3-3), the collection efficiency, η, is inversely proportional to Q_{in}.

4. Results and Discussion

4.1 Performance of electrometer

4.1.1 Zero-point measurement:

Fig. 3 shows the readouts of the TPAE during warm-up. For reference, the temperatures of the hot and cold disks are also given in the figure. At the initial time, the zero-point of the electrometer was approximately 57 fA, and the temperatures of the hot and cold disks were both 22.3°C. During warm-up, the temperatures of the plates rose at different rates, establishing the increasing temperature gradient. The hot and cold disk temperatures eventually stabilized at 61.40°C (±0.20°C) and 48.15°C (±0.15°C), respectively. In the meantime, the TPAE readout reduced and finally stabilized at -20.68fA (±2fA). The warm-up of the prototype took approximately 40 minutes to establish the temperature gradient of 265 K/cm (±7 K/cm). A higher temperature gradient can be realized by increasing the heating and cooling powers.
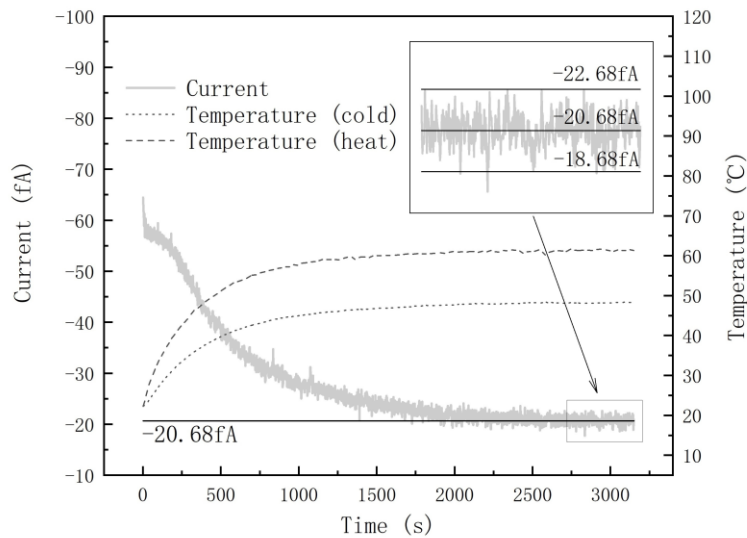
Fig 3. The readout of TPAE during the warm-up process (particle-free air was used).

Assuming that particles in the sample gas are singly charged, sampling flowrate is Q, and e is elementary charge, the current I can be calculated as eNQ, where N is the particle number concentration. If $Q = 0.3$ L/min, $N = 1250(\# \cdot cm^{-3})$ per fA, the $\pm 2fA$ fluctuation is the equivalent of ± 2500 # cm^{-3}

4.1.2 Response time measurement

Fig. 4 shows the readout of the TPAE experiencing a step change in the number concentration of soot particles at sampling flowrates of 0.3 L/min (a) and 0.6 L/min (b). For reference, the readout of the TSI aerosol electrometer is also included. It is found that the trends of the TPAE and the TSI aerosol electrometer are consistent. Ideally, $I_{\mathrm{TPAE}}(t)$ equals to $\eta I_{3068}(t)$, $t > 0$, where $\eta = I_{\mathrm{TPAE}}(t)/I_{3068}(t)$ is the particle collection efficiency of the TPAE. The efficiency data as a function of time is also included in the figure. During the time periods of $0 \sim 30$s and $140 \sim 170$s with the sampling flowrate at 0.3 L/min, and the periods of $0 \sim 16$s and $80 \sim 100$s with 0.6 L/min, the current readouts were very low (close to zero), resulting in an unsteady η. Conversely, during the time periods of $40 \sim 120$s and $25 \sim 70$s for the flowrates of 0.3 and 0.6 L/min, respectively, the collection efficiency was constant. This is because the number concentration of the test particles was stable and the η was kept constant (i.e., 98.5% (± 1%) for 0.3 L/min case, and 56.0% (± 1%) for 0.6 L/min case).
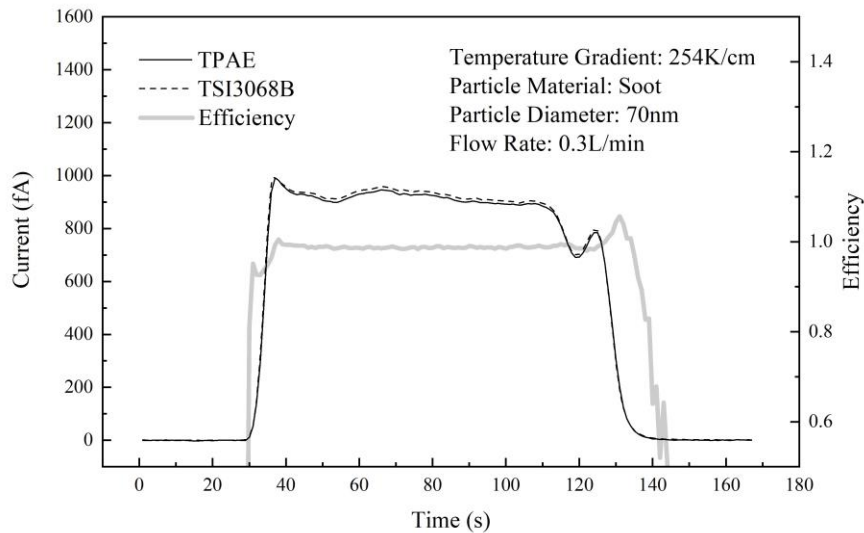
(a) sampling flow: 0.3 L/min
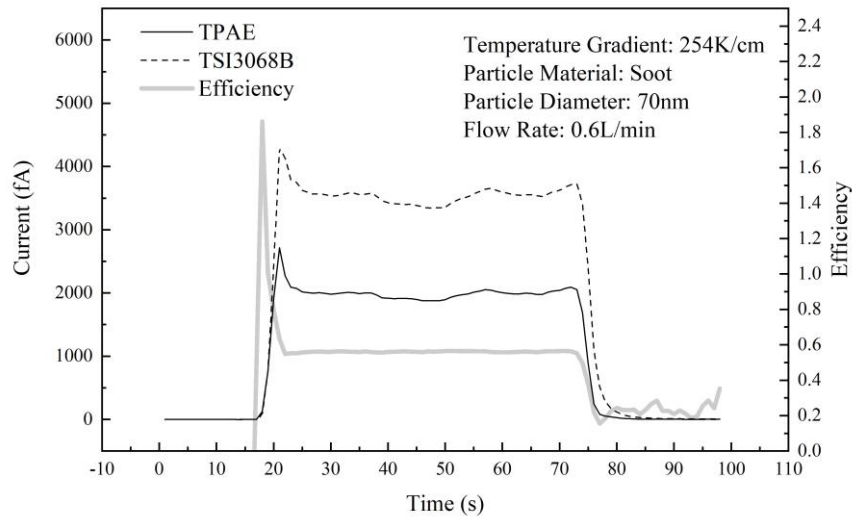
(b) sampling flow: 0.6 L/min

Fig 4: The readout of TPAE in response to the step particle concentration change. The readout of TSI aerosol electrometer was also included for reference.

For the sampling flowrate of 0.3 L/min, the collection efficiency during the time period of 30 ~ 40s was less than 98.5%, indicating the response of the TPAE to a step rise in the particle concentration is slower than that offered by the TSI aerosol electrometer. The same observation can be found in the time period of 125 ~ 135s. However, the response time difference between the two electrometers is within one second. A similar conclusion can be reached examining the case with the sampling flowrate of 0.6 L/min. Therefore, the response of the TPAE can keep up with that of TSI aerosol electrometer within 1s. The response of the AEs can be characterized by the times for the reading to rise from 10% to 90% of the final readout, and for the reading reducing from 90% of an initial reading to 10% when subjected to a step change in the particle concentration, i.e., $t_{10\text{-}90}$ and $t_{90\text{-}10}$, respectively. The values of $t_{10\text{-}90}$ and $t_{90\text{-}10}$ calculated from Fig. 4. Are summarized in Table 2. Compared to the response times of the TSI3068B, the TPAE response time is almost the same as that of the TSI3068B at the flowrate of 0.3 L/min, and slightly faster at the flowrate of 0.6 L/min.

Table 2: Response time of TDAE and TSI3068B

Parameters	0.3L/min		0.6L/min	
	TPAE	TSI3068B	TPAE	TSI3068B
$t_{10\text{-}90}$	3.96s	3.83s	1.83s	2.08s
$t_{90\text{-}10}$	6.59s	6.63s	2.65s	3.52s

4.1.3 Readout linearity between two aerosol electrometers
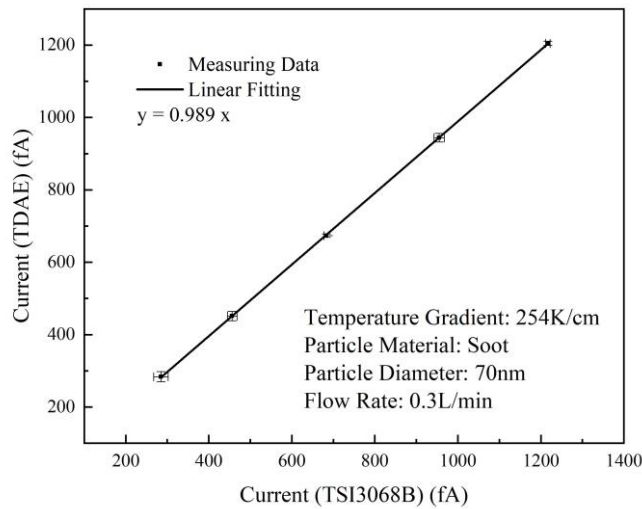
(a) sample flow: 0.3L/min
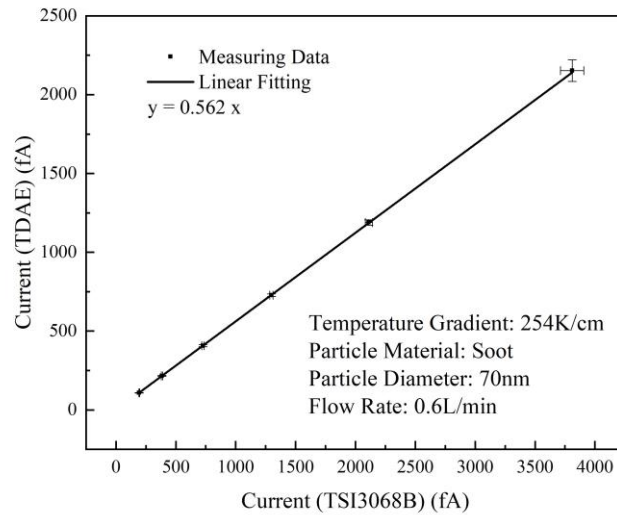
(b) sample flow: 0.6L/min

Fig 5: Linear correlation between the readouts of TPAE and TSI aerosol electrometer

Figure 5 shows the readout correlation between the TPAE and TSI aerosol electrometers at the sampling flow rates of 0.3 and 0.6 L/min. A linear correlation between the two readouts was observed. In the case of 0.3 L/min (Fig. 5a), the best linear fitting resulted in a slope of 0.989. Note that the slope of this best linear fitting is the particle collection efficiency of the TPAE. It is because the collection efficiency of the TSI aerosol electrometer is close to 100%. Similarly, in the case of 0.6 L/min (Fig. 5b), the best fitting with a straight line obtained a slope of 0.562. The observation above of reduced particle collection efficiency with the increase of sampling flowrate is expected according to Eq. (3-3).

4.2 Investigation of TPAE particle collection efficiency

4.2.1 Effect of temperature gradient
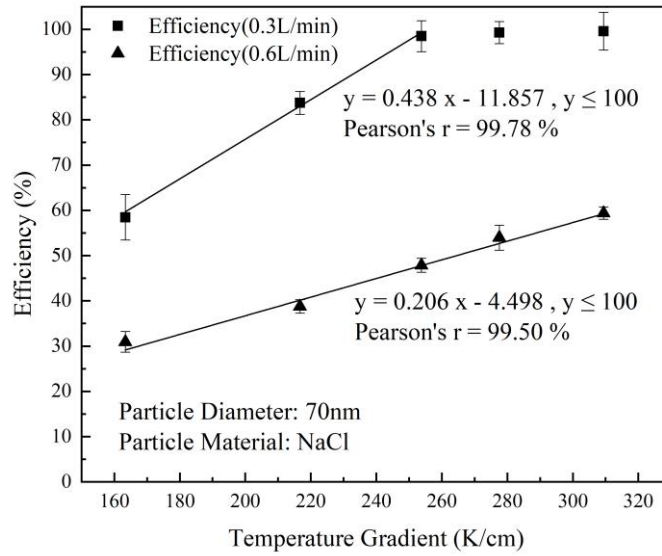
Fig. 6: Calibration of collection efficiency and temperature gradient

Fig. 6 shows the particle collection efficiency of the TPAE as the function of the temperature gradient for NaCl particles of 70 nm in size, and at the sampling flow rates of 0.3 and 0.6 L/min. It is found that, for the 0.3 L/min flowrate, the collection efficiency linearly increases with the increase of the temperature gradient, and the collection efficiency reached ~ 100% when the gradient exceeded 264 K/cm. For the flowrate of 0.6 L/min, the collection efficiency is again linearly increased with the increase of temperature gradient within the test gradient range, but did not reach ~100% collection efficiency. The above experimental observation is consistent with that given by Eq. (3-3)

4.2.2 Effects of sampling flow rate and particle size
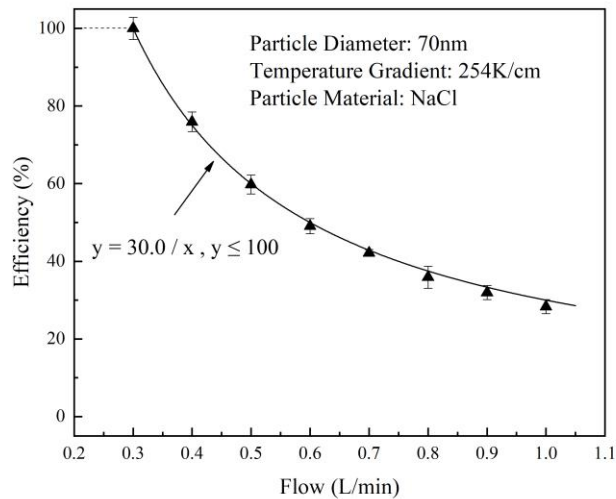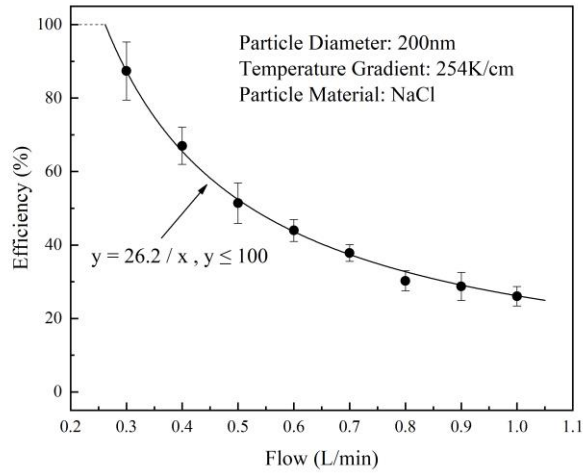
(b) 200nm particles

295   **Fig 7: The particle collection efficiency of TPAE as the function of sampling flowrate at two different NaCl particles sizes (i.e., 70 and 200 nm)**

In this part of the experiments, the temperature gradient in the TPAE was set at 264 K/cm and NaCl particles of 70 and 200 nm in sizes were selected for this investigation. The sampling flowrate of the TPAE was varied from 0.3 to 1.0 L/min. Fig. 7 shows the measured particle collection efficiency of the TPAE as a function of the sampling flow rate for a given particle size.

300   As expected, for a given particle size, the collection efficiency was reduced as the sampling flow rate increased, and the reduction characteristics followed what was expected from Eq. (3-3), i.e., the collection efficiency is inversely proportional to the sampling flow rate (Q_{in}). As a result, the products of $(\eta \cdot Q_{in})_{70nm}$ and $(\eta \cdot Q_{in})_{200nm}$ remained $30.0 \pm 1.7\% \cdot$ L/min, and $26.2 \pm 2.0\% \cdot$ L/min, respectively.
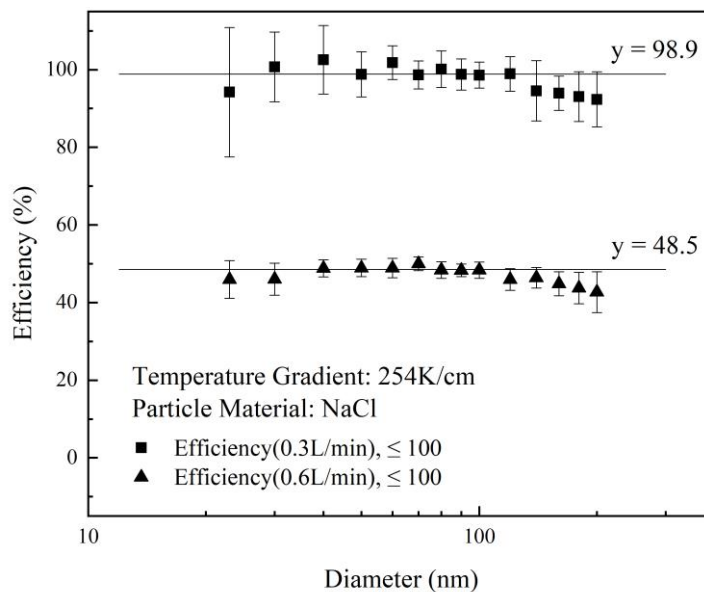
305   **Fig 8: The measured TPAE particle collection efficiency as a function of the NaCl particle size for the sampling flow rate of 0.3 and 0.6 L/min.**

The effect of particle size on the TPAE collection efficiency is given in Fig. 8 for the sampling flow rates of 0.3 and 0.6 L/min. For particle sizes less than 120nm, the efficiency was ~ 98.9% and ~ 48.5% for both 0.3 and 0.6 L/min flow rates, respectively.

310   As the particle diameter increased, the collection efficiency of the TPAE was slightly decreased, which is consistent with the thermal precipitation velocity obtained in previous works (Beresnev et al., 2019, Wang et al., 2012). According to Eq. (3-4), the larger the particle size, the lower the thermal precipitation velocity.

4.2.3 Collection efficiency for soot particles
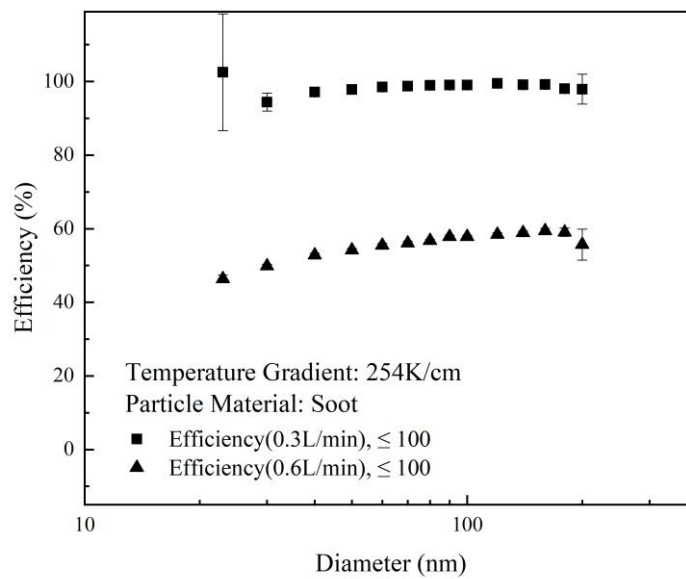
315   **Fig 9: The measured TPAE particle collection efficiency as a function of the soot particle size for the sampling flow rate of 0.3 and 0.6 L/min.**

In addition to NaCl particles, soot particles were also used for the collection efficiency measurement. The electrical mobility size of soot particles ranging from 23 to 200 nm was tested. The measured particle collection efficiency as a function of electrical mobility size at the temperature gradient of 264 K/cm and the sampling flow rates of 0.3 and 0.6 L/min is given in

320   Fig. 9. A slightly positive correlation of the collection efficiency with the electrical mobility size was found. As shown in Fig. 9, the collection efficiency at the sampling flow rate of 0.3 L/min achieved ~100% as the particle size increased. In the case of 0.6 L/min, the collection slightly increased with the increase of electrical mobility particle size. The experiment results are consistent with that reported by Beresnev et al. (2019). It is known that soot particles are agglomerates of primary particles. Their thermal precipitation velocity cannot be estimated using Eq. (3-4) because the equation assumes particles are solid and

325   in a spherical shape. For soot particles, their density and thermal conductivity are very different from the bulk material, and

their shapes are not spherical. The effect of particle shape may play an important role in the thermal deposition of soot particles, because the collection efficiency of 23 nm soot particles at the sampling flow rate of 0.6 L/min was 46.4%, which approximately equals to that of NaCl particles (45.9%). This may be because at small mobility sizes, soot agglomerates are structured only by a few of the primary particles.

5. Conclusion

A new type of aerosol electrometer, the thermal precipitation aerosol electrometer (TPAE), has been developed in this work. Its overall performance has been experimentally calibrated and compared with that of a reference (TSI aerosol electrometer). The design of the TPAE integrates the thermal precipitation chamber with a micro-current measurement circuit. The precipitation chamber is in the disk-to-disk configuration and its temperature gradient is established by heating the top disk and cooling the bottom disk. Air cooling was used in the TPAE instead of the liquid cooling used in previous works. A current probe (i.e., solid cupper pin) in the micro- current measurement circuit was attached to the cold disk (converting it into an electrode), which was enclosed by the top disk and cooling flow chamber to minimize the potential interference from the ambient electromagnetic waves.

For the performance calibration, the zero-point of the prototype was first measured during warm-up to the stable operation. The zero-point current converged to 20.68fA (±2fA) for the TPAE. The measurement of the TPAE response time was also conducted and compared to that of the reference. It was found that the difference between both electrometers was within one second. A linear correlation between the readouts of both aerosol electrometers was also confirmed.

The collection efficiency of the TPAE was experimentally investigated. It was found that the effects of temperature gradient, sampling flow rate and particle size on the particle collection efficiency are consistent with those obtained from previous models and experimental data. In addition to NaCl particles, soot particles were also used in the collection efficiency measurements. It was found that the collection efficiency of soot particles was slightly increased as the mobility particle sizes increased at a given setting of sampling flow rate and temperature gradient, which is different from that of NaCl particles. This observation is probably due to the fact that soot particles in large mobility sizes are agglomerates of the primary particles instead of solid, spherical particles (which is what is assumed by the models), and that soot agglomerates have different density and thermal conductivities compared with those of the bulk materials.

Data availability.

Requests for all data in this study and any questions regarding the data can be directed to Shipeng Kang (spkang@mail.ustc.edu.cn).

Competing interests.

The authors declare that they have no conflict of interest.

Special issue statement.

This article is part of the special issue "In-depth study of the atmospheric chemistry over the Tibetan Plateau: measurement, processing, and the impacts on climate and air quality (ACP/AMT inter-journal SI)". It is not associated with a conference.

Author contributions.

SK: Writing – original draft, Visualization, Data curation and analysis; TY: Sample collection, Project administration; YY: Resources, Data validation; JW: Experiment; HG: Writing – review; JL: Conceptualization, Supervision; DC: Writing – review & editing, Experiment, Formal analysis.

Acknowledgements.

This research was supported by the National Natural Science Foundation of China (42005108), the Science and Technological Fund of Anhui Province (2008085MD116), Major Subject of Science and Technology of Anhui Province (202003a07020005), Strategic Priority Research Program of the Chinese Academy of Sciences (XDA23010200), the National Engineering Laboratory for Mobile Source Emission Control Technology (NELMS2020A09) and the HFIPS Director's Fund (Nos. BJPY2021A04).

References

Alas, H. D. C., Weinhold, K., Costabile, F., Di Ianni, A., Müller, T., Pfeifer, S., Di Liberto L., Turner, J. R., and Wiedensohler, A.: Methodology for high-quality mobile measurement with focus on black carbon and particle mass concentrations, Atmospheric Measurement Techniques, 12, 4697-4712, doi:10.5194/amt-12-4697-2019, 2019.

Beresnev, S. A., Vasiljeva, M. S., and Kochneva, L. B.: Motion of fractal-like aggregates: particle settling velocity and thermophoresis, Atmospheric and Oceanic Optics, 32, 528-533, doi:10.1134/s102485601905004x, 2019.

Bredl, J., and Grieve, T. W.: A thermal precipitator for the gravimetric estimation of solid particles in flue gases, Journal of Scientific Instruments, 28, 21-23, 1951.

Dixkens, J., and Fissan, H.: Development of an electrostatic precipitator for off-line particle analysis, Aerosol Science and Technology, 30, 438-453, 1999.

380 Etzion, Y., and Broday, D. M.: Highly resolved spatiotemporal variability of fine particle number concentrations in an urban neighborhood, Journal of Aerosol Science, 117, 118-126, doi: 10.1016/j.jaerosci.2018.01.004, 2018.

Faxvog, F. R., and Roessler, D. M.: Mass concentration of diesel particle emissions from photoacoustic and opacity measurements, Aerosol Science and Technology, 1, 225-234, doi:10.1080/02786828208958590, 2007.

Fierz, M., Houle, C., Steigmeier, P., and Burtscher, H.: Design, calibration, and field performance of a miniature diffusion size classifier, Aerosol Science and Technology, 45, 1-10, doi:10.1080/02786826.2010.516283, 2011.

385 Giechaskiel, B., Wang, X., Horn, H. G., Spielvogel, J., Gerhart, C., Southgate, J., Jing, L., Kasper, M., Drossinos, Y., Krasenbrink, A.: Calibration of condensation particle counters for legislated vehicle number emission measurements, Aerosol Science and Technology, 43, 1164-1173. doi:10.1080/02786820903242029, 2009.

Held, A., Orsini, D. A., Vaattovaara, P., Tjernström, M., and Leck, C.: Near-surface profiles of aerosol number concentration and temperature over the Arctic Ocean, Atmospheric Measurement Techniques, 4, 1603-1616, doi:10.5194/amt-4-1603-2011, 390 2011.

Hillemann, L., Zschoppe, A., Caldow, R., Sem, G. J., and Wiedensohler, A.: An ultrafine particle monitor for size-resolved number concentration measurements in atmospheric aerosols, Journal of Aerosol Science, 68, 14-24, doi:10.1016/j.jaerosci.2013.10.007, 2014.

Intra, P., and Tippayawong, N.: Development and evaluation of a Faraday Cup Electrometer for measuring and sampling 395 atmospheric ions and charged aerosols, Particulate Science and Technology, 33, 257-263, doi:10.1080/02726351.2014.952392, 2014.

Keskinen, J., Pietarinen, K., and Lehtimaki, M.: Electrical Low-Pressure Impactor, Journal of Aerosol Science, 23, 353-360, 1992.

Kethley, T. W., Gordon, M. T., and Orr, C.: A thermal precipitator for aerobacteriology, Science, 116, 368-369, 1952.

400 Kheirkhah, P., Baldelli, A., Kirchen, P., and Rogak, S.: Development and validation of a multi-angle light scattering method for fast engine soot mass and size measurements, Aerosol Science and Technology, 54, 1083-1101, 2020.

Liu, B. Y. H., and Pui, D. Y. H.: On the performance of the electrical aerosol analyzer, Journal of Aerosol Science, 6, 249-264, 1975.

Liu, Q., Liu, D., Chen, X., Zhang, Q., Jiang, J., and Chen, D.-R.: A cost-effective, miniature electrical ultrafine particle sizer 405 (mini-eUPS) for ultrafine particle (UFP) monitoring network, Aerosol and Air Quality Research, 20, 231-241, doi:10.4209/aaqr.2018.11.0427, 2020.

Molgaard, B., Birmili, W., Clifford, S., Massling, A., Eleftheriadis, K., Norman, M., Vratolis S., Wehner, B., Corander J., Hameri, K., and Hussein, T.: Evaluation of a statistical forecast model for size-fractionated urban particle number concentrations using data from five European cities, Journal of Aerosol Science, 66, 96-110, 410 doi:10.1016/j.jaerosci.2013.08.012, 2013.

Seol, K. S., Tsutatani, Y., Camata, R. P., Yabumoto, J., Isomura, S., Okada, Y., Okuyama, K., and Takeuchi, K.: A differential mobility analyzer and a Faraday Cup Electrometer for operation at 200-930 Pa pressure, Journal of Aerosol Science, 31, 1389-1395, 2000.

Talbot, L., Cheng, R. K., Schefer, R. W., and Willis, D. R.: Thermophoresis of particles in a heated boundary-layer, Journal of Fluid Mechanics, 101, 737-758, 1980.

Tammet, H., Mirme, A., and Tamm, E.: Electrical aerosol spectrometer of Tartu University, Atmospheric Research, 62, 315-324, 2002.

Tsai, C.-J., and Lu, H.-C.: Design and evaluation of a plate-to-plate thermophoretic precipitator, Aerosol Science and Technology, 22, 172-180, doi:10.1080/02786829408959738, 1995.

Wang, B., Ou, Q., Tao, S., and Chen, D.-R.: Performance study of a disk-to-disk thermal precipitator, Journal of Aerosol Science, 52, 45-56, doi:10.1016/j.jaerosci.2012.04.004, 2012.

Wang, B., Tao, S., and Chen, D.-R.: A cylindrical thermal precipitator with a particle size-selective inlet, Aerosol Science and Technology, 46, 1227-1238, doi:10.1080/02786826.2012.704097, 2012.

Wang, X., Grose, M. A., Avenido, A., Stolzenburg, M. R., Caldow, R., Osmondson, B. L., Chow, J. C., and Watson, J. G.: Improvement of Engine Exhaust Particle Sizer (EEPS) size distribution measurement – I. Algorithm and applications to compact-shape particles, Journal of Aerosol Science, 92, 95-108, doi:10.1016/j.jaerosci.2015.11.002, 2016.

Wang, X., Grose, M. A., Caldow, R., Osmondson, B. L., Swanson, J. J., Chow, J. C., Watson, J. G., Kittelson, D. B., Li, Y., Xue, J., Jung, H., and Hu, S.: Improvement of Engine Exhaust Particle Sizer (EEPS) size distribution measurement – II. Engine exhaust particles, Journal of Aerosol Science, 92, 83-94, doi:10.1016/j.jaerosci.2015.11.003, 2016.

Yang, Y., Yu, T., Zhang, J., Wang, J., Wang, W., Gui, H., and Liu, J.: On the performance of an Aerosol Electrometer with enhanced detection limit, Sensors (Basel), 18, doi:10.3390/s18113889, 2018.

Yang, Y., Yu, T., Zhang, J., Wang, W., Gui, H., Du, P., and Liu, J.: Design and evaluation of an Aerosol Electrometer with low noise and a wide dynamic range, Sensors (Basel), 18, doi:10.3390/s18051614, 2018.